Potential and limitations of convection-permitting CNRM-AROME climate modelling in the French Alps

Diego Monteiro, Cécile Caillaud, Raphaëlle Samacoïts, Matthieu Lafaysse, Samuel Morin

ORIGINAL ARTICLE

Journal Section

Potential and limitations of convection-permitting CNRM-AROME climate modelling in the French Alps

Diego Monteiro[1*] | Cécile Caillaud[2] | Raphaëlle Samacoïts[3] | Matthieu Lafaysse[1] | Samuel Morin[1,2]

[1]Univ. Grenoble Alpes, Université de Toulouse, Météo-France, CNRS, CNRM, Centre d'Etudes de la Neige, 38000 Grenoble, France

[2]CNRM, Météo-France, CNRS, Université de Toulouse, Toulouse, France

[3]Météo-France, Direction de la Climatologie et des Services Climatiques, Toulouse, France

Correspondence
CNRM/CEN, 1441 rue de la piscine, F-38400 St Martin d'Hères
Email: diego.monteiro@meteo.fr

Funding information

Convection permitting climate modelling is a promising avenue for climate change research and services especially in mountainous regions. Work is required to evaluate the results of high resolution simulations against relevant observations, and put them in a broader context against coarser resolution modelling frameworks. Here we evaluate numerical simulations with the convection permitting regional climate model CNRM-AROME ran at 2.5 km horizontal resolution over a large pan-Alpine domain in the European Alps, using either the ERA-Interim or climate model output as boundary conditions.

This study analyses annual and seasonal characteristics of 2m temperature, total precipitation, solid fraction of precipitation and snow depth at the scale of the French Alps under past and future climate conditions. The results are compared with the local reanalysis S2M, and raw or adjusted, with the ADAMONT method, simulations of the regional climate model CNRM-ALADIN driven either by the ERA-Interim reanalysis or the CNRM-CM5 global climate model.

The study highlights generally similar differences in past and future climate between the datasets, as well as obsta-

cles to the use of some CNRM-AROME outputs as they stand. These consist of excessive accumulation of snow on the ground above 1800 m a.s.l., as well as lower temperature values at same elevations than the S2M reanalysis and the ADAMONT-adjusted outputs.

Besides these obstacles, CNRM-AROME simulations present several advantages compared to the raw CNRM-ALADIN outputs. Among them, a significantly smaller cold bias, more realistic values of accumulated precipitations, as well as a better representation of the spatial variability of the different variables investigated, which always stand closer to the reference data than in the CNRM-ALADIN outputs. As suggested by many studies, CNRM-AROME could even produce more realistic accumulated precipitations at high elevation than the S2M reanalysis taken as our reference and consequently than the ADAMONT-adjusted projections, but the lack of a reliable set of high-resolution observations at high elevation remains an obstacle to their evaluation.

KEYWORDS

CP-RCM, Mountain, Climate change, AROME, Snow

1 | INTRODUCTION

Over the past decades, climate projections applied to assess regional climate change mainly came from the combined use of general circulation model (GCM) dynamically downscaled by regional climate models (RCM). International efforts such as EURO-CORDEX have lead to the production of 12 km resolution simulations from multiple GCM/RCM pairs and their use for various applications (Jacob et al., 2014; Beniston et al., 2018). Within this framework, the use of adjustment methods and statistical downscaling are necessary to exploit them, which is especially true in mountainous environnements where the complex topography leads to significant deviations between model outputs and observational datasets (Hock et al., 2019). For example, the statistical adjustment method ADAMONT was applied to the Alps and Pyrenees using the SAFRAN meteorological reanalysis as a reference observation dataset for processing multiple EURO-CORDEX GCM/RCM pairs (Verfaillie et al., 2017, 2018; Evin et al., 2019). However, such approaches neglect several key physical processes playing a role in shaping climate change patterns in mountainous regions and the assumption of the stationarity of the bias corrections between present and future climate remains questionable.

Convection permitting regional climate models (CP-RCMs) are increasingly considered as a potent step forward in climate change studies, holding amongst others promising potentials in mountain regions Prein et al. (2013). Indeed, such models have shown added-value concerning the representation of precipitation over complex terrain, whether

it concerns their spatial or temporal characteristics, in particular on the sub-daily time scale, particularly in summer (Keller et al., 2016). The representation of extremes, as well as rainfall accumulation in high relief against lower-resolution RCMs such as ALADIN (Spiridonov et al., 2005) which do not resolve explicitely deep convection, have also been demonstrated (Lind et al., 2016; Ban et al., 2021).

In this context, the high-resolution AROME numerical weather prediction model (Seity et al., 2011) is now used for climate simulations. The first applications of the AROME model as a climate model (also referred to as CNRM-AROME) were carried out to analyze the evolution of extreme precipitation in the South-East of France under climate change (Déqué et al., 2016). More recently, climate simulations using AROME with a 2.5 km horizontal grid spacing were conducted over the pan-Alpine domain. This was carried out within the CP-RCMs multi-model study project defined in the Flagship Pilot Study « Convection » of EURO-CORDEX described by Coppola et al. (2020). CNRM-AROME simulations have, inter alia, demonstrated their added-value in their capacity to represent Mediterranean extreme precipitation events in the fall season (Fumière et al., 2020; Caillaud et al., 2021).

Although studies including CNRM-AROME simulations have mainly focused on the precipitation added-value of CP-RCMs, Lüthi et al. (2019) have shown that a CP-RCM model (COSMO) was able to improve remarkably the representation of the Swiss alpine snow cover components compared to coarser resolution simulations, in line with previous studies of snow cover within coarser resolution RCM (Terzago et al., 2017; Matiu et al., 2020) conclusions, which outlined a clear added-value of using higher resolution climate models to represent snow related variables over mountainous regions.

Increased horizontal resolution provided by the new generation of convection permitting climate models could therefore allow for approaching debated questions such as elevation dependent warming (Kotlarski et al., 2015; Rottler et al., 2019), changes in the intensity of convective precipitations in mountain areas (Giorgi et al., 2016) or assess climate change impacts at high elevations. Indeed, some studies have illustrated the interest of using CP-RCM in projected climate change by comparing them to coarser RCM over the alpine region. For example, Lüthi et al. (2019) showed that COSMO refined and enhanced projected reduction in snow water equivalent. Pichelli et al. (2021) showed that an ensemble of CP-RCM compared to a coarser RCM ensemble can lead to a different change in the sign of the heavy precipitation intensity change over some regions. Prior to the study of these complex climate processes, one needs to assess the capacities of such models to represent climate characteristics over the targeted area. The added value and limitations of CP-RCMs need to be quantified thoroughly, in a context where the scientific community faces strong expectations from a number of societal spheres, especially in the context of extreme weather events and related natural disasters in mountain regions. Such an analysis is also a prerequisite for any use of the output of such models as a forcing dataset for impacts studies in weather-sensitive sectors or applications (avalanche hazard, ski tourism, glacier evolution, water resources, impacts on ecosystems etc.) which are currently mostly addressed, in state-of-the-art studies, using adjusted GCM/RCM ensembles (e.g Spandre et al., 2019; Morin et al., 2021; Zekollari et al., 2019). The main questions addressed here are :

- What are the seasonal climate characteristics of the outputs from CP-RCM CNRM-AROME over the French Alps ?
- Are these outputs bringing added-value compared to the results fo the CNRM-AROME coarser resolution driving RCM ?
- What are the differences between future changes in CNRM-AROME output across the 21^{st} century, and results of statistically adjusted projections, both driven by the same GCM/RCM pair ?

This study provides a case study of the CNRM-AROME CP-RCM output over the French Alps, focusing on the surface air temperature at 2 m, total amount and solid fraction of precipitation and snow depth at annual and seasonal integration time scales, as a function of location and elevation. The evaluation is carried out using multiple datasets, aggregated over climatically homogeneous geographical entities within which atmospheric and snow cover variables are allowed to vary with elevation, thereby providing a novel and robust approach to compare observations and climate model outputs in mountainous areas. Analyses of CNRM-AROME output are carried in past and futur climate, and compared to the local reanalysis S2M, its raw driving RCM ALADIN, as well as statistically adjusted RCM ALADIN using the ADAMONT method.

2 | MATERIAL AND METHODS

Several datasets were used in this study, originating from model simulations and observations. Figure 1 provides an overview of all the datasets employed and combined, along with their corresponding time coverage. Individual models and datasets are described in detail in section 2.1.

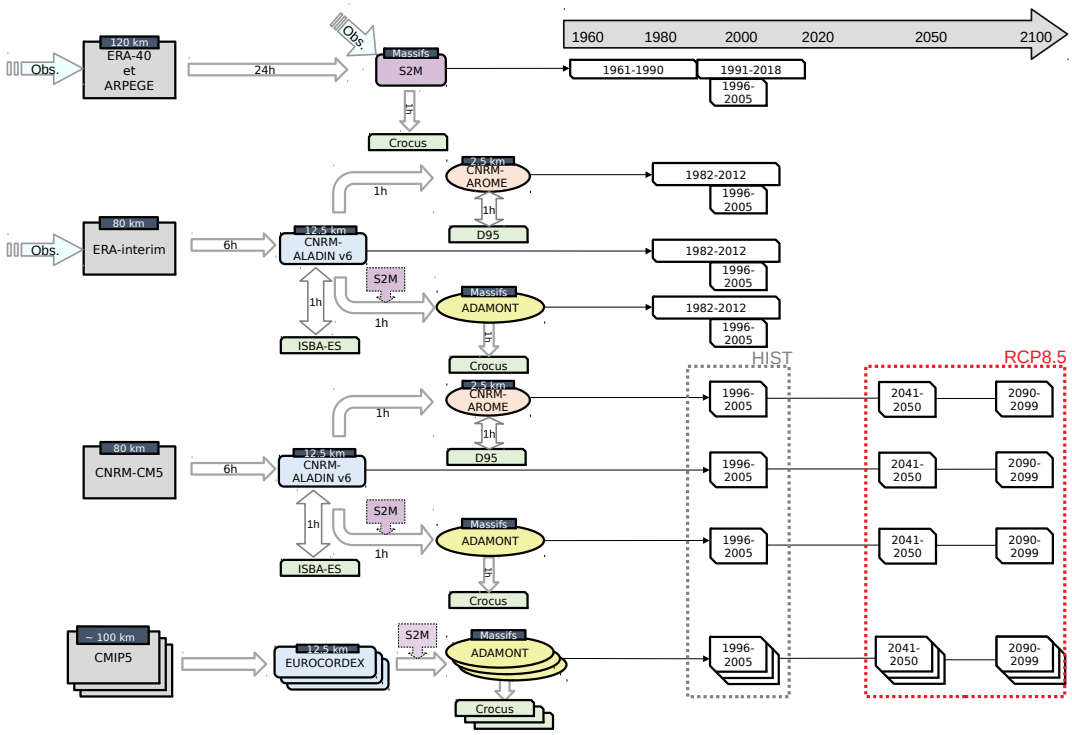

FIGURE 1 Overview of the datasets used in this study. In grey, the global reanalysis ERA-Interim or general circulation models (GCMs); in blue, regional climate models (RCMs) driven by global datasets; in orange, dynamically downscaled RCM (CP-RCM); in yellow, statistically downscaled RCM using the method ADAMONT ; in violet, reference dataset, here the regional reanalysis S2M ; in green, snow cover models providing snow cover variables through coupled or offline simulations. The wide arrows start from the models used to drive further, higher resolution models, with their forcing frequencies indicated in hours. Double wide arrows indicate the presence of a coupling between two components. The thin arrows point to the periods for which the datasets are used in this study.

2.1 | Data

2.1.1 | SAFRAN-Crocus (S2M) reanalysis

The SAFRAN reanalysis (Durand et al., 2009; Vernay et al., 2021) results from a combination of multiple meteorological data coming from different observation sources (automatic stations, manual observations, radiosoundings ...) and a synoptic guess from ERA-40 (Uppala et al., 2005) for the 1958-2002 period, and from the operational global NWP model ARPEGE since 2002. It covers primarily in French mountain regions, using 23 massifs, in the French Alps, as its basic geographical entity. For each massif, with a surface area of about 1000 km^2, meteorological and snow cover conditions are assumed to depend only on the elevation, with data provided by 300 m-spaced elevation bands. The SAFRAN reanalysis provides hourly values for air temperature, relative humidity or specific, liquid and solid precipitation, wind speed and direction, incoming short and longwave radiation from 1958 to 2020. As part of the SAFRAN - SURFEX/ISBA-Crocus - MEPRA reanalysis (S2M) (Vernay et al., 2019), atmospheric fields from SAFRAN are used to drive the snow cover model Crocus (Vionnet et al., 2012), thereby providing daily snow cover information on the same spatial scale. In this study, we only use snow cover simulations on flat terrain, and the S2M reanalysis is used as a reference observation dataset, bringing together available information in a consistent and integrated manner. Indeed, at the elevations where observations are available, S2M reanalyses do not suffer from systematic biases in meteorological variables when compared to observations (due to the analysis process), and do not suffer from systematic biases in simulated snow depths (Vernay et al., submitted). However, it is known that S2M is affected by several intrinsic limitations such as severe temporal heterogeneities of input observations affecting the quality of long-terms trends (Vernay et al., submitted), a likely underestimation of precipitation at high elevation (typically above 3000 m (Vionnet et al., 2019)), and a reported underestimation of incident solar radiation compared to in-situ observations (Quéno et al., 2020).

2.1.2 | CNRM-ALADIN - RCM

We use the CNRM-ALADINv6 (ALADIN in the following) regional climate model (see Nabat et al. (2020) for further details concerning its parametrizations schemes and configurations), which uses a 12.5 km horizontal grid spacing over a large pan-European domain, 91 vertical levels and a 450 s internal time step. It is hydrostatic, which involves the parametrisation of deep convection, using the PCMT (Prognostic Condensates Microphysics and Transport) scheme (Piriou and Guérémy, 2016). The coupling with the land surface modeling system SURFEX8 (Decharme et al., 2019) includes the snow cover model ISBA-ES, using a 12-layers snowpack discretisation scheme (Boone and Etchevers, 2001; Decharme et al., 2016), including an ad'hoc option for limiting unrealistic snow accumulation at high elevation. ALADIN was driven by the ERA-Interim (Dee et al., 2011) reanalysis for the evaluation simulations, as well as the CNRM-CM5 GCM output (Voldoire et al., 2013) for the historical and scenario (RCP8.5) simulations. In this work, the ALADIN outputs are used as they stand, but also as the intermediate forcing dataset for the CNRM-AROME model and as input to the statistical adjustment method ADAMONT.

2.1.3 | Statistical adjustment ADAMONT

The ADAMONT method (Verfaillie et al., 2017) is a statistical adjustment method used to adjust spatially and disaggregate daily outputs from RCM, using a reference dataset at hourly resolution. It uses a quantile mapping approach, meaning that the quantile distribution of each variable from the RCM is corrected based on the quantile distribution of a reference dataset over an common past period. It then creates correction tables for each adjusted points, which

are then applied to the output of the climate projections of the same RCM.

In this study, the ADAMONT method was applied to the outputs from CNRM-ALADIN, as well as 19 other GCM/RCM model pairs from the EURO-CORDEX ensemble, using the S2M meteorological fields (see Section 2.1.1) as reference observations. The output from the ADAMONT-adjusted GCM/RCM model output was used to drive corresponding Crocus snow cover simulations.

2.1.4 | CNRM-AROME - CP-RCM

The CNRM-AROME (AROME in the following) model corresponds to the numerical weather forecast model AROME developed at CNRM (Seity et al., 2011; Termonia et al., 2018), used operationally since December 2008 at Météo-France. This study relies on simulations carried out with CNRM-AROME (cycle 41t1) at 2.5 km horizontal grid spacing Caillaud et al. (2021); Ban et al. (2021); Pichelli et al. (2021). This version of the model was the one used operationally for NWP at Météo-France from 2015 to 2018 (see Termonia et al. (2018) for further details concerning its parametrizations schemes and configurations).

A key difference of this kilometric resolution model is its dynamic core, the non-hydrostatic spectral version used by the ALADIN model (Bénard et al., 2010), with a semi-lagangian advection scheme and a semi-explicit time discretisation. This makes it possible to explicitly resolve deep convection. CNRM-AROME includes a coupling with SURFEX 7.3, which provides a detailed representation of continental surfaces with an high resolution topography. The snowpack model used in CNRM-AROME is the single layer D95 model (Douville et al., 1995). It models the snowpack as one layer which evolves according to snowfall, evaporation/sublimation and melting. The albedo is a decreasing function of age of the snow, and the density is treated as a prognostic variable, which increases exponentially with time and decreases with new snowfall (Martin, 2005).

2.2 | Methods

2.2.1 | Geographical domain

The study focuses on the French Alps, using AROME simulations ran over the pan-Alpine domain (ALP-3), as shown on Figure 2. CNRM-ALADIN simulations used in this study were performed for two different domains called MED-11 and EUR-11 (see `https://cordex.org` for further details concerning the domains). The French Alps are in both cases located at the center of the domain, which leads to negigible differences in the topographical representation of the French Alps.

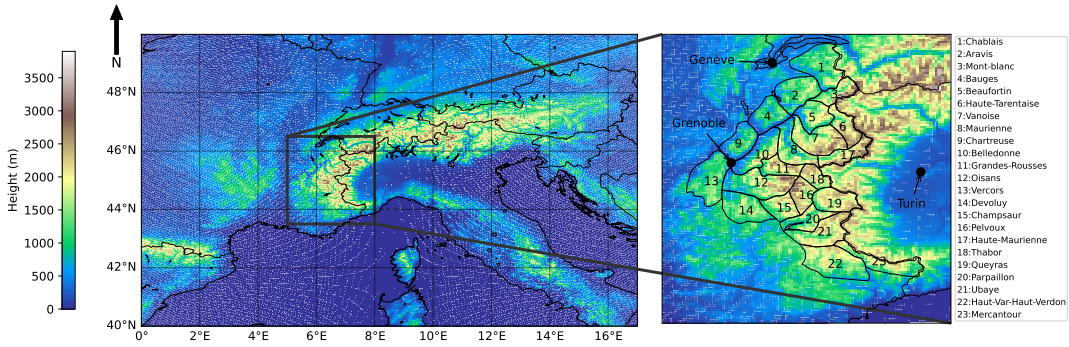

FIGURE 2 Geographical setting of the study. On the left side, AROME topography over the ALP-3 domain. On the right side, a zoom in of AROME topography covering the French Alps, on which the contours of the S2M massifs are superimposed.

2.2.2 | Aggregation of AROME and ALADIN simulation over the S2M massifs

We used the S2M geometry, by massifs and elevation bands, as a reference for carrying out comparisons and evaluations. For each modelling system used, grid points were attributed to each massif according to their geographical coordinates and grouped by elevation slices into 300 m width slices, by gathering data for grid points from 150 m below to 150 m above for each 300 m elevation band.

We focus on the elevation bands from 900 m to 2700 m (i.e., including grid points from 750 m to 2850 m elevation), where a sufficient number of grid points are represented (see Figure 3), from ALADIN and AROME simulations.

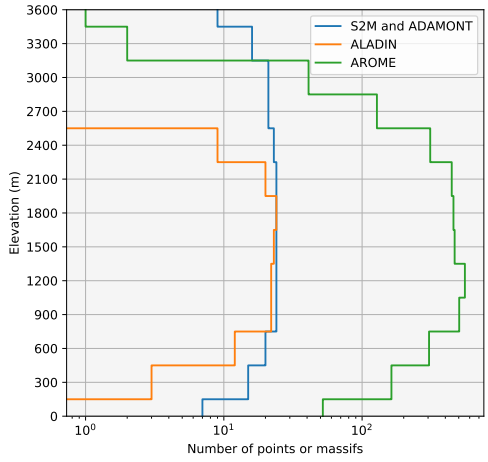

FIGURE 3 Altitudinal repartition of the number of points/massifs per 300 m elevation band (z ± 150 m) for AROME and ALADIN, and massifs for S2M and ADAMONT.

Note that for Figures 5 and 7 (as well as figures A1 to A4), data points are displayed for all ALADIN and AROME grid

points within the elevation band investigated (1800 m +/-150 m for Figures 5 and 7, 1200 m and 2400 m ± 150 m for Figures A1 to A4) , in order to depict potential intra-massif geographical patterns. Grid points were also displayed outside the domain investigated to provide a more complete sight of the spatial coverage of grid points within the corresponding elevation band.

2.2.3 | Description of indicators and spatial aggregation

We computed indicators characterizing the main features of mountain regions climatology, based on 2m air temperature, total precipitation, solid precipitation fraction and snow depth, at seasonal (September to November SON for fall, December to February DJF for winter, March to May MAM for springtime and June to August JJA for summer) and annual time scales. We focused, in particular, on seasonal and annual mean air temperature, total precipitation, mean solid precipitation fraction and snow depth. Note that annual values for mean solid precipitation fraction and snow depth were taken for the time period from December to May (winter and springtime).

For all indicators described above, we computed spatial averages covering the entire French Alps, taking the average over the 23 massifs (equal weight given to each massif, given their comparable individual surface area), after a first aggregation of gridded datasets within each massif and elevation band. This provides robust estimates of the meteorological and snow conditions for the entire French Alps in a consistent and comparable way, although this masks out spatial variability within the region when using such aggregated values. Several results are provided here at 1800 m elevation (representing the data contained in the 1800 m ± 150 m band), covering most of the French Alps presenting for all datasets a large number of massifs and points (see Figure 3) and relevant to study climate variability and long term in meteorological and snow conditions in the French Alps (Durand et al., 2009). Results for other elevations are provided and discussed when relevant, and included in supplements.

2.2.4 | Implementation of the simulations and evaluation strategy

Figure 1 provides an overview of all the datasets used in this study and the time periods relevant to each of them. We used ALADIN simulations driven by two different global driving datasets: ERA-Interim (for the evaluation period 1982-2012) and CNRM-CM5 (for the historical period 1996-2005 and future time periods 2041-2050 and 2090-2099 using the RCP8.5 greenhouse gas concentration scenario).In both cases and for the same time period, ALADIN simulations were used as an intermediate driving RCM for AROME simulations over the ALP-3 domain (see Figure 2). ALADIN simulations driven by ERA-Interim were performed over the MED-CORDEX (MED-11) domain (Ruti et al., 2016) using spectral nudging (von Storch et al., 2000; Radu et al., 2008). Spectral nudging enables to constrain large-scale conditions inside the nesting domain, and therefore to remain closer to the driving dataset. For further details concerning the spectral nudging applied to the ALADIN simulations used in this study, see Nabat et al. (2020).

ALADIN simulations driven by CNRM-CM5 were carried out over the EURO-CORDEX domain (EUR-11). For climate projections, AROME simulations were produced over 10 years time slices 1996-2005, 2041-2050 and 2090-2099. This high resolution simulation framework is in line with the choice done within the EURO-CORDEX Flagship Pilot Study Convection (Coppola et al., 2020). All ALADIN model runs, as well as 19 other GCM/RCM pairs from the EURO-CORDEX ensemble, were used as input to the ADAMONT statistical adjustment method using S2M meteorological fields as reference meteorological datasets over the 1980-2012 period. In this case, one grid point for each RCM was used for each massif (the closest to the barycenter of each massif), similar to the approach taken by Verfaillie et al. (2018).

3 | RESULTS

We first describe AROME multi-annual seasonal characteristics over the evaluation period, spanning from 1982 to 2012, across different elevations, averaged over the French Alps, as well as at finer spatial scale to look at geographical patterns over the different regions. AROME simulations are compared to ALADIN raw outputs, and the S2M reanalysis. Then, change across the 21^{st} century (differences between end and beginning of century) for the RCP8.5 are investigated using similar indicators, and compared to ALADIN raw outputs and statistically adjusted ALADIN outputs with ADAMONT method. The analysis also includes a summary table of annual mean values at 1800 m, covering all datasets at all periods available, allowing the comparison of the effects of using different driving datasets.

3.1 | Past climate conditions

We first focus on the comparison of the various datasets for the time period from 1982-2012, for all indicators at the seasonal scale. Figure 4 shows the elevation profiles, per season, averaged over the 1982-2012 period for the ERAi/ALADIN/AROME (AROME) and ERAi/ALADIN (ALADIN) simulations, as well as the S2M reanalysis (S2M). ADAMONT profiles are not displayed in the figures below. Indeed, by design, the differences between ADAMONT and S2M are very small for all variables represented, but larger differences between AROME, ALADIN and S2M can be seen. In the Figure 5, the three first rows display the 30 years average values for all the grid points included within the 1800m elevation band (1800m +/-150m), inside and also outside the S2M massif border for ALADIN and AROME. The two last rows show the differences of the 30 average values between ALADIN and S2M, AROME and S2M.

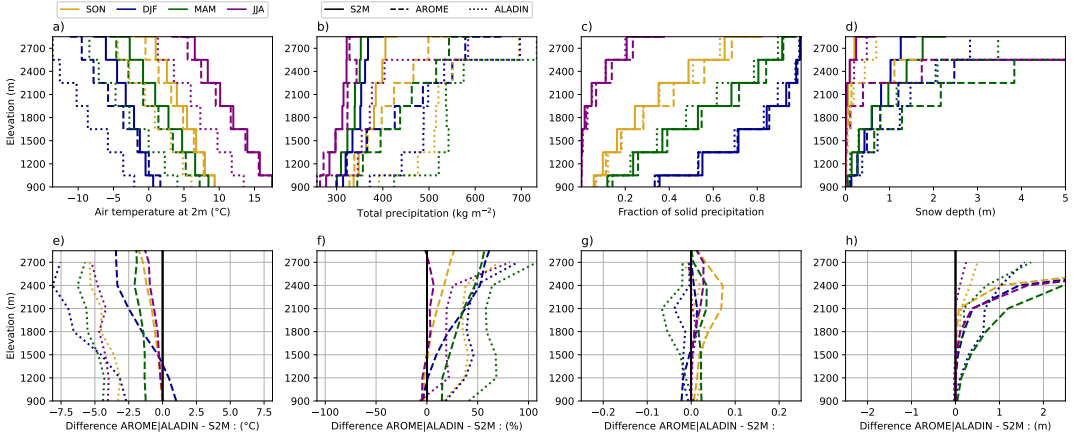

FIGURE 4 Time-averaged elevation profiles over the period 1982-2012, for 4 variables at the seasonal scale: a) air temperature, b) total precipitation, c) solid precipitation fraction, and d) snow depth. On the second line, (e), (f), (g), (h), the respective differences between the datasets AROME - S2M (dashed) and ALADIN - S2M (dotted).

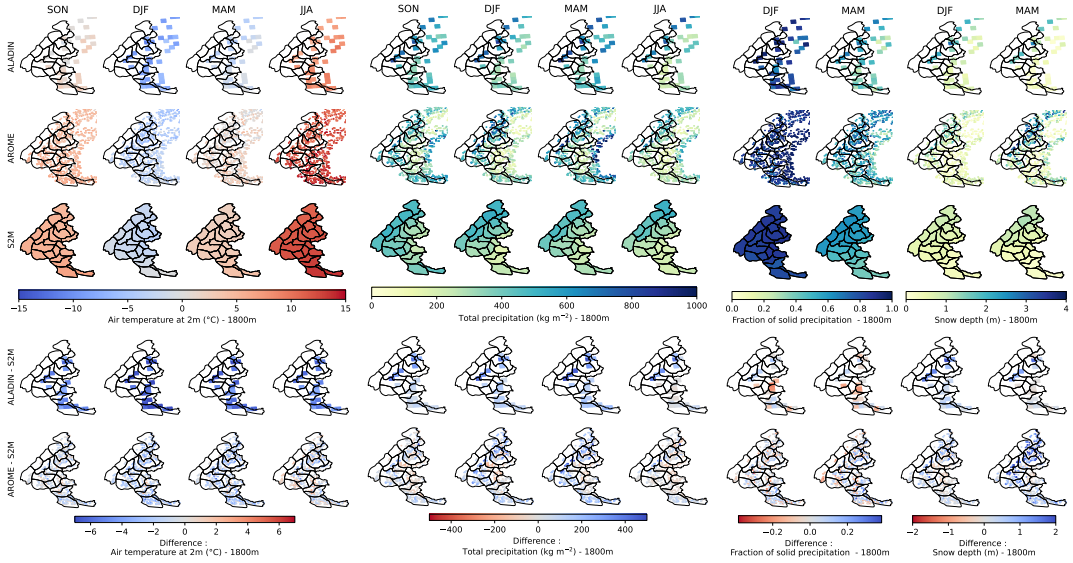

FIGURE 5 Simulation results at 1800 m elevation (representing grid point values within the 1800 m ± 150 m elevation band for AROME and ALADIN, inside and outside the S2M massif border) for the three datasets and their seasonal values over the period 1982-2012, for 4 variables: air temperature, total precipitation, solid precipitation fraction, and snow depth. Columns correspond to the different seasons. The three first rows present the different models : ALADIN, AROME and S2M, while the fourth and the fifth ones correspond to the differences between ALADIN and S2M, and AROME and S2M, respectively.

Air temperature

On Figure 4.a-e, AROME and ALADIN simulations generally show lower temperatures than S2M for all seasons, and the differences increase with elevation to various extents depending on the season. We note that for all seasons, the altitudinal profiles of the differences Figure 4.e are similar for AROME and ALADIN, with a shift of around 3 degrees warmer for AROME outputs, making them closer to the reanalysis. The differences and their increases with elevation are most pronounced in winter, with a difference of +1°C at 900 m for AROME, -2.5°C for ALADIN, reaching -3.5°C at 2700 m between AROME and S2M, -7.5°C between ALADIN and S2M (Figure 4.e). These increases are smaller in spring, with a difference of -1.5°C at 1200 m reaching -2°C at 2700 m for AROME, similar for ALADIN but 3°C colder. AROME and ALADIN summer and autumn profiles Figure 4.a exhibit the smallest differences and increases above 1500 m, from 0°C at 900 m to -1/-1.5°C at 2700 m for AROME and from -3/-4°C at 900 m to -5°C at 2700 m for ALADIN.

Figure 5 shows similar geographical patterns between S2M and both AROME and ALADIN simulations. The two last rows showing the differences of AROME and ALADIN against S2M data confirm that both datasets provide lower temperature values than S2M, particularly in winter (down to almost -6°C difference at some grid points), although several grid points show higher values in AROME than in S2M. This is observed at all elevations, except below 1200 m elevation where AROME simulations show higher temperature values than S2M.

Total precipitation

Figure 4.b shows that precipitation amounts generally increase with elevation for S2M, ALADIN and AROME, and are larger in the ALADIN simulations than AROME and AROME than S2M, both for all elevations, with differences increasing with elevation. This behaviour is particularly marked in winter and spring, with seasonal accumulations at 2700 m 60% higher in AROME than in S2M, and up to 100% for ALADIN compared to S2M (see Figure 4.f). From September to May in AROME outputs, and for all seasons in ALADIN, a strong elevation gradient can be observed, resulting in accumulated values up to 80% larger at 2700 m than at 900 m. This gradient is less pronounced in the S2M data, regardless of the season, as well as in AROME summer data, and is more continuous in AROME simulations than in ALADIN profiles (Figure 4.b), almost vertical between 1500 m and 2400 m.

The annual distribution of precipitation is also different between the datasets. For the S2M data, the larger precipitation total occurs during the autumn period (Figure 4.b), in spring for ALADIN, while AROME results indicate more precipitations in spring for altitudes ranging from 900 m to 1800 m, and in winter above 2100 m.

In terms of geographical pattern, total precipation values show similarities across the three datasets at 1800 m (also valid at other elevations 1200 m and 2400 m, see Figures A1 and A2), with higher values on the north-western massifs, whereas inner and southern parts of the French Alps receive less precipitations for most seasons, except in autumn, where the southern part receive almost as much precipitation as the northern part, probably due to the occurence of mediterranean storms at this season. Higher precipitation values in AROME and ALADIN outputs, compared to S2M, are also displayed in Figures 4 and 5, although AROME exhibits systematically lower precipitation values than S2M in the inner Alps. ALADIN and AROME simulate extremely high precipitation amounts at very few grid points around the Mont-Blanc massif for all season at intermediate and high elevation (Figures 5, A1 and A2), with values that can reach 200% of S2M values.

Fraction of solid precipitations

The fraction of solid precipitation, shown on Figure 4-c-g, displays only small differences between the AROME, ALADIN and S2M dataset, not exceeding 0.06. We note based on Figure 4-g that AROME outputs show larger solid fraction for all seasons above 1500 m, whereas ALADIN shows the contrary, and that both show their maximum differences with S2M within the 1500 m to 2400 m elevation bands. Figure 5 shows a similar pattern at 1800 m (and other intermediate levels) for the three datasets, with more precipitations falling as snowfall in the northern part of the Alps, whereas the southern part receives less solid precipitation in autumn and spring. Values for winter and summer are relatively homogenous, with almost only snowfall and rainfall, respectively.

Snow depth

Snow depth values simulated by the AROME show exceptionally high values from 2100 m and above, compared to S2M rising above several meters on average (see Figures 4d-h). ALADIN simulates lower values of snow depth than AROME, although the differences with S2M can be as much as double at high elevations. Figure 5 shows that at 1800 m elevation, AROME and S2M snow depth values are in broad agreement in terms of overall pattern. Figure 5 also shows that exceptionally high snow depth values are only found for few grid points at 1800 m. In fact, even at elevation above 1800 m (see Figure A2), only few grid points keep spurious values of snow depths (also in fall season, not shown here), whereas the others show no accumulation.

The exceptionally high AROME snow depth values are too large to be explained by differences in precipitation, solid precipitation fraction and temperature alone. Some hypotheses are explored in the discussion, in order to explain these outliers.

3.2 | Climate projections

In this section, we describe projected changes over the 21^{st} century based on 10 years averages (2090-2099 minus 1996-2005) for AROME, ALADIN and ADAMONT, as well as differences between simulations (AROME – ADAMONT and ALADIN - ADAMONT) for the same periods (1996-2005 and 2090-2099).

Figure 6.a-d and Figure 6.i-l respectively display simulated changes between 1996-2005 and 2090-2099 for AROME and ADAMONT and for AROME and ALADIN, for the four variables investigated, as a function of elevation.

Figure 6.e-h and Figure 6.m-p respectively display the differences between AROME and ADAMONT, and between AROME and ALADIN outputs, for 1996-2005 and 2090-2099 , for the four variables investigated, as a function of elevation

In Figure 7, the three first rows display the simulated change over the 21^{st} century (between 1996-2005 and 2090-2099) for all the grid points included within the 1800 m elevation band (1800m +/-150 m), inside and also outside the S2M massif boundaries (for ALADIN and AROME). The two lowermost rows show the differences of simulated change between 1996-2005 and 2090-2099 between ALADIN and ADAMONT, and AROME and ADAMONT, respectively

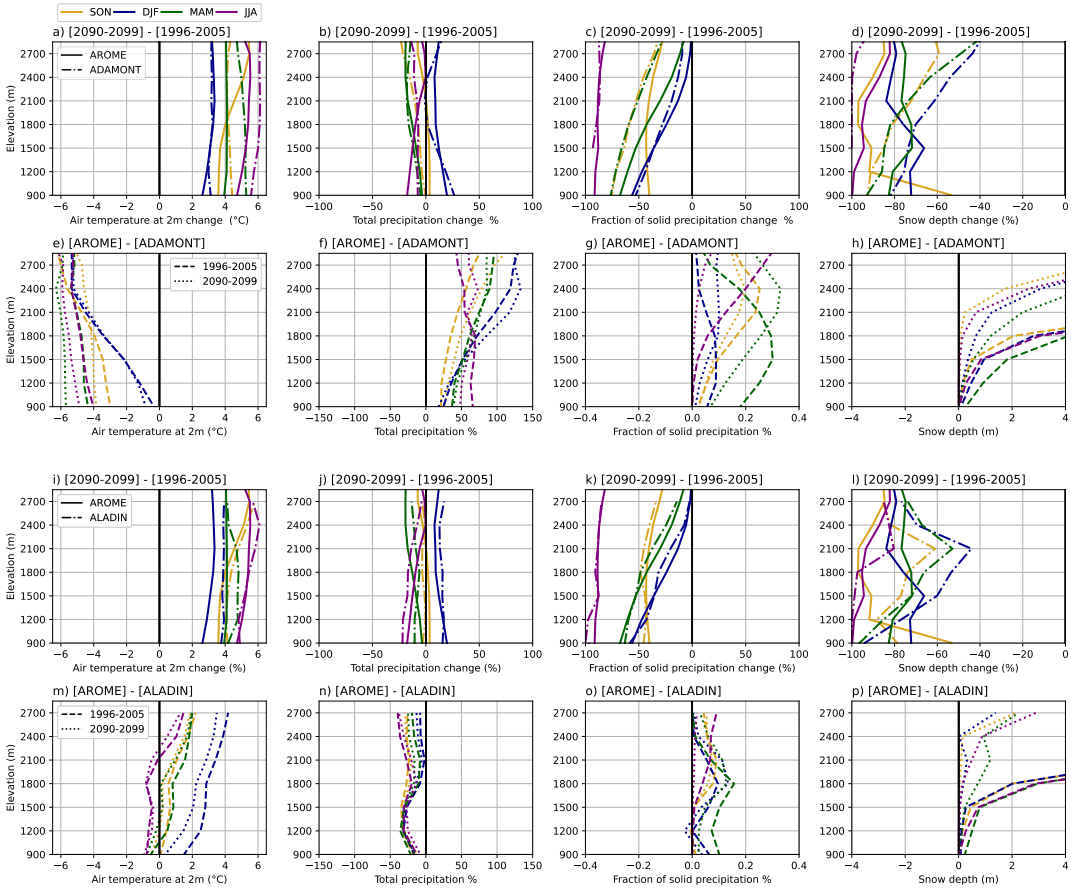

FIGURE 6 Altitudinal profiles, by season, for 4 variables: a-e-i-m) air temperature at 2m, b-f-j-n) total precipitation, c-g-k-o) solid fraction of precipitation, and d-h-l-p) snow depth. The first (third) line is the difference between the averages of the end-of-century (2090-2099) and beginning-of-century (1996-2005) periods, for the AROME data in solid line, and the ADAMONT (ALADIN) data in dashed line. The second (fourth) line represents the difference between the average of the AROME and ADAMONT (ALADIN) data for each of the periods at the beginning (dashed) and end of the century (dotted).

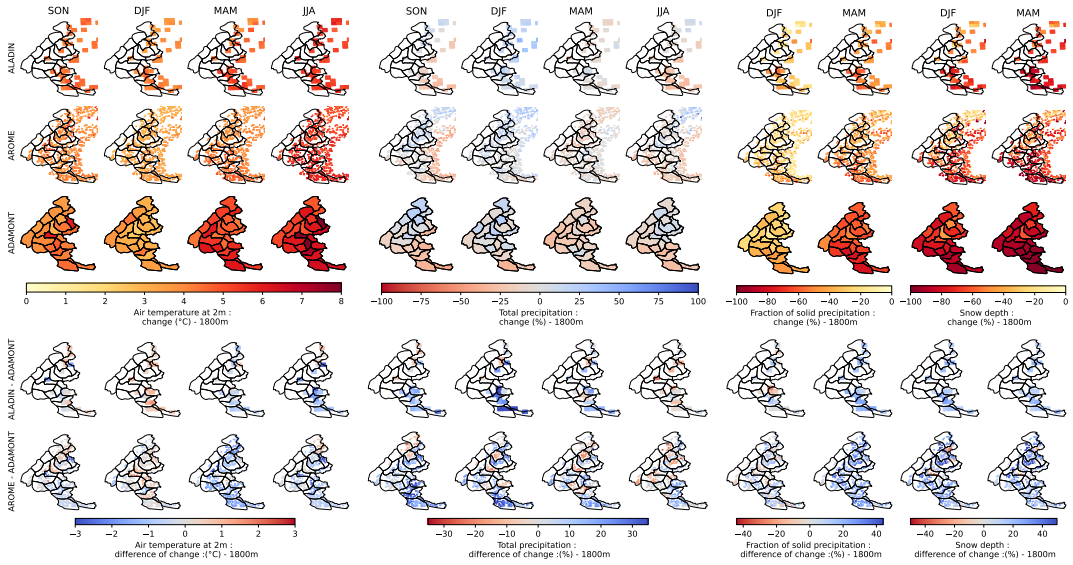

FIGURE 7 Simulation results at 1800 m (representing grid point values within the 1800 m ± 150 m elevation band for AROME and ALADIN, inside and outside the S2M massif borders) for the three datasets ALADIN, AROME and ADAMONT. Values of the three first rows correspond to the change over the 21^{st} century (differences between the seasonal averages of the end-of-century (2090-2099) and beginning-of-century (1996-2005) periods), for 4 variables: air temperature at 2m, total precipitation, solid fraction of precipitation, and snow depth. Columns correspond to the different seasons. The two last rows show the differences between ALADIN and S2M change values, and AROME and S2M change values, respectively.

Air temperature

The air temperature changes between the end (2090-2099) and beginning (1996-2005) of the 21st century, displayed on Figure 6-a-i, show small altitudinal variations over the represented elevation range, with the same values for AROME and ADAMONT in winter (+3°C, 6-a), and 1°C warmer for ALADIN (6-i), which corresponds to the least warming season. For AROME, ALADIN and ADAMONT, the summer season shows the greatest mean warming, from 5.5°C to 6°C for ADAMONT, and around 1°C lower for AROME and ALADIN, regardless of the elevation. For ADAMONT, spring is the season that undergoes the most marked warming after summer, for all elevations, whereas AROME and ALADIN simulates that from 1800 m upwards, autumn shows a stronger warming reaching +5°C at 2700 m, almost similar to the summer value. Overall, AROME simulates the lower warming over the 21st century, on average around 1°C lower than ADAMONT for spring and summer and than ALADIN for winter and spring.

Figure 7 displays the temperature change geographical pattern at 1800 m, which is generally homogeneous for fall and winter seasons in AROME and ALADIN outputs, whereas in spring and summer the warming is, on average, 1°C larger in the south than in the north. The main differences between ALADIN, AROME and ADAMONT datasets, in terms of temperature change, are mainly related to the spatial heterogeneity in ADAMONT temperature changes. In spring and summer, almost all grid points show a smaller temperature change for AROME and ALADIN than for ADAMONT, whereas in winter season in the inner Alps, AROME shows higher temperature change than ADAMONT.

In terms of the differences between temperatures profiles, Figure 6-e shows that differences between AROME and ADAMONT CNRM-CM5 driven are similar to the ERAi driven ones but exacerbated (see Figure 4-f). However, differences between AROME and ALADIN Figure 6-m show for all seasons lower cold deviations that can be seen on

Figure 4-f. This is explained by the fact that simulations CNRM-CM5 driven for AROME are 3°C colder than ERAi driven simulations for the 1996-2005 period at 1800 m (see Table 1), whereas a slight warming of 0.7°C is observed for ALADIN ones.

| Total precipitation

Changes over the 21st century are shown in Figure 6-b-j and are rather small and heterogeneous in their seasonal distribution. Total winter precipitation values in AROME and ALADIN at the end of the century are on average 15% higher than at the beginning of the century (from +10% to +20% depending on elevation), a change that is only found at low elevations for ADAMONT.

Spring and summer profiles (Figure 6-b-j) show rather similar trends for all datasets, with a general drying, slighty oscillating along the elevations, from 0 to 20%. Fall season is the most contrasted between simulations, with no change at all elevations in AROME and ALADIN, whereas ADAMONT presents similar trends that for summer or spring, around 10-15%.

Figure 7 shows that precipitation changes are similarly distributed at 1800 m elevation between AROME and ADAMONT, both AROME and ADAMONT presenting much more discrepancy with ALADIN. Values for spring and summer seasons show almost only negative changes at all elevations. In the fall and winter, AROME and ADAMONT changes are roughly similar, with increases in the northern part and decreases in the southern part at all elevations in the fall, but only at intermediate elevations for winter season (with increases almost everywhere at low and high elevations, see Figures A3 and A4).

The differences between precipitation changes across the 21st century in AROME and ADAMONT depend strongly on the massif, which is mostly due to the inter-massif heterogeneity in precipitation changes in ADAMONT.

Total precipitation amounts in AROME and ADAMONT climate projections Figure 6-f-n are larger than in ADAMONT output, and the differences increase with elevation, similar to simulations for ERAi driven (see Figure 4-b-f). However, the differences are larger when AROME and ALADIN are driven by CNRM-CM5 (from 50 to 70% in autumn and summer to 125 to 150% of the ADAMONT totals in winter) than when forced by ERAi (at most 60% to 80% of the S2M or ADAMONT totals).

| Fraction of solid precipitation

Figure 6-c-k shows a decrease in the solid fraction of precipitation regardless of the season and elevation, with similar changes in ADAMONT, ALADIN and AROME. In winter, the relative differences between the end and beginning of the century are around 50% at low elevation, then decrease in elevation, becoming almost zero at 2700 m. Changes are strongest in summer, where the average solid precipitation fraction reach zero at low elevation and is reduced by 90% at high elevation, for both datasets. Changes are also large in autumn and spring, with a 50-75% reduction at lower elevations, and 35% at 2700 m. These strong decreases in the fraction of solid precipitation are directly related to the temperature increases.

Figure 7 shows the changes in the fraction of solid precipitation at 1800 m elevation, with a stronger decrease in the southern part than the northern part, especially in autumn. The relative decrease is larger in ADAMONT results than AROME and ALADIN for most of the grid points.

Snow depth

Snow depth values at 1800 m and above in AROME and above 2400 m ALADIN projections are exceptionally high (Figure 6-h-p) compared to ADAMONT, similar to past simulations comparing AROME or ALADIN and S2M. These high values of snow depth may explain the different behaviours of change across the 21^{st} century between ADAMONT and AROME above 1500 m Figure 6-d-l) and between ADAMONT and ALADIN above 2100 m Figure 6-l). Indeed, whereas snow depth values show a relative decrease decreasing with elevation in ADAMONT, AROME and ALADIN show an increase with elevation starting from the elevation where they present high snow depth values which prevents any meaningful comparison to other projections or an analysis of future changes at these elevations.

Nevertheless, an analysis can be carried out at low and intermediate elevations (shown at 1800 m elevation on Figure 7). At lower elevation (1200 m elevation on Figure A3), there is a relatively homogenous general decrease in snow depth values, whereas at intermediate (for AROME and ADAMONT and high elevations (for ADAMONT) relative changes are larger in the southern part of the Alps. At low and intermediate levels (below 1800 m), the decrease in snow depth values is larger in ADAMONT than in AROME for most of the grid points.

Overall comparison between all datasets

Period	Dataset // Variable	Temperature at 2 m (°C) -annual mean-	accumulated precipitations (kg m^{-2}) -annual mean-	Fraction of solid precipitation -DJFMAM mean-	Snow depth (m) -DJFMAM mean-
1961-1990	S2M	4.3±0.6	1390±200	0.73±0.07	0.71±0.22
1991-2018	S2M	4.8±0.7	1390±170	0.67±0.06	0.56±0.18
1982-2012	S2M	4.6±0.5	1380±260	0.68±0.05	0.59±0.25
	ERAi/ALADIN	-0.8±0.6	1910±200	0.63±0.07	0.99±0.19
	ERAi/ALADIN/ADAMONT	4.7±0.5	1360±210	0.67±0.06	0.64±0.22
	ERAi/ALADIN/AROME	3.6±0.7	1580±180	0.69±0.06	1.01±0.17
1996-2005	S2M	4.6±0.5	1380±320	0.68±0.05	0.54±0.20
	ERAi/ALADIN	-0.8±0.5	1850±250	0.64±0.08	0.96±0.11
	ERAi/ALADIN/ADAMONT	4.7±0.5	1300±240	0.67±0.06	0.61±0.19
	ERAi/ALADIN/AROME	3.6±0.6	1540±210	0.69±0.04	1.00±0.11
	CNRM-CM5/ALADIN	-0.1±0.7	2630±300	0.73±0.03	1.50±0.60
	CNRM-CM5/ALADIN/ADAMONT	4.9±0.70	1330±290	0.66±0.06	0.60±0.40
	EUROCORDEX/ADAMONT	Q_{20} : 4.7 Q_{50} : 4.8 Q_{80} : 4.9	Q_{20} : 1260 Q_{50} : 1330 Q_{80} : 1350	Q_{20} : 0.65 Q_{50} : 0.66 Q_{80} : 0.68	Q_{20} : 0.52 Q_{50} : 0.57 Q_{80} : 0.60
	CNRM-CM5/ALADIN/AROME	0.7±0.8	2190±260	0.87±0.06	3.89±0.22
2041-2050	CNRM-CM5/ALADIN	1.2±0.6	2740±240	0.63±0.06	1.16±0.28
	CNRM-CM5/ALADIN/ADAMONT	6.3±0.6	1400±260	0.56±0.06	0.39±0.17
	EUROCORDEX/ADAMONT	Q_{20} : 5.9 Q_{50} : 6.5 Q_{80} : 7.0	Q_{20} : 1300 Q_{50} : 1400 Q_{80} : 1530	Q_{20} : 0.51 Q_{50} : 0.55 Q_{80} : 0.58	Q_{20} : 0.32 Q_{50} : 0.38 Q_{80} : 0.44
	CNRM-CM5/ALADIN/AROME	1.9±0.5	2300±120	0.76±0.02	2.42±0.07
2090-2099	CNRM-CM5/ALADIN	4.5±0.6	2560±180	0.45±0.09	0.60±0.40
	CNRM-CM5/ALADIN/ADAMONT	9.7±0.7	1280±190	0.41±0.09	0.15±0.21
	EUROCORDEX/ADAMONT	Q_{20} : 9.2 Q_{50} : 9.9 Q_{80} : 10.7	Q_{20} : 1040 Q_{50} : 1170 Q_{80} : 1350	Q_{20} : 0.28 Q_{50} : 0.31 Q_{80} : 0.38	Q_{20} : 0.06 Q_{50} : 0.10 Q_{80} : 0.13
	CNRM-CM5/ALADIN/AROME	5.0±0.8	2130±140	0.58±0.05	1.13±0.05

TABLE 1 Summary table of annual values (fraction of solid precipitation and snow depth values are averaged over the December to May period) and their interannual standard deviations at 1800 m elevation for the four variables analysed in this study, averaged over each period, for each of the datasets shown in Figure 1. The values in the "EUROCORDEX/ADAMONT" row correspond to the median (Q_{50}) and quantiles Q_{20} and Q_{80} of the multi-annual means of the ADAMONT-adjusted EUROCORDEX set consisting of 19 GCM/RCM pairs.

Table 1 provides annual mean values (for air temperature and total precipitation) and december to april values (for fraction of solid precipitations and snow depth) at 1800 m, over the French Alps for all datasets shown in Figure 1. All these values are averaged over their corresponding period in the table. This makes it possible to carry out a compact and quantitative comparison, complementary to the analysis performed in the previous sections and corroborating the results described previously, and summarized below:

- Lower temperature, in general, in ALADIN and AROME compared with ADAMONT or S2M, with a larger difference in the raw ALADIN outputs.
- Higher amounts of total precipitation in ALADIN and AROME, compared to ADAMONT or S2M, also more pronounced in ALADIN outputs.
- The fraction of solid precipitation is generally close or a bit higher in AROME and ALADIN than in S2M or ADAMONT datasets.
- Spurious high snow depth values are found in AROME simulation results, also found in ALADIN, but to a lesser extent and at higher elevation.

All the datasets are available for the period 1996-2005, which makes it possible to compare the influence of the ERA-Interim and CNRM-CM5 forcing in a similar climate context for both AROME and ALADIN simulations. Using the GCM CNRM-CM5 reinforces the features described above, with colder values (except for ALADIN), greater amount of precipitation, higher proportion of precipitations falling as solid, and therefore larger snow cover. This difference could partly be due to the specificity of the GCM CNRM-CM5, leading to wetter and colder simulation compared to ERA-Interim, but also to the specific characteristics of the ALADIN RCM, whose specific influence is limited due to the spectral nudging in the run driven by ERAi. Natural climate variability, not entirely smoothed out in a 10 years average could have some influence, with a chronology of meteorological events imposed by CNRM-CM5, forming a colder and wetter sequence than that of ERAi.

The median and quantiles of the multi-annual means of the EURO-CORDEX ensemble adjusted by ADAMONT indicate that the CNRM-CM5/ALADIN simulations are slightly colder and with higher precipitation than the median of the ensemble, especially at the end of the century. This results in a higher proportion of solid precipitation and a higher snow accumulation, even if this GCM/RCM pair remains overall close to the median of the ensemble for most of its characteristics.

4 | DISCUSSION

This study analyzes a series of complementary climate simulations covering the French Alps, providing several opportunities to identify and discuss limitations and benefits of the CP-RCM AROME.

| Temperature differences between simulations

| ALADIN vs. AROME

There are large temperature differences, for all seasons, over all the elevations investigated, ranging from -1 to -5°C, between ALADIN and AROME. Furthermore AROME results show significantly lower temperature values than S2M (past climate) and ADAMONT (future climate), particularly in winter, with differences increasing with elevation.

These features are in line with numerous studies evaluating the EURO-CORDEX ensembles of simulations over an extended alpine domain. Indeed, large negative temperature differences between the RCMs and reference datasets over the Alpine region have been highlighted in Kotlarski et al. (2014); Smiatek et al. (2016); Terzago et al. (2017); Frei et al. (2018). These studies showed that ALADIN simulations, using comparable versions to those used in this study, lie systematically among the models showing the strongest cold biases, regardless of the season considered.

AROME simulations show a much lower «cold bias» compared to ALADIN , for all elevations and seasons. This behaviour was also observed in Lind et al. (2020) over Scandinavia, comparing ALADIN and AROME simulations, but to a much lesser extent. The differences in results between the studies could be due to climatic differences inducing different model behaviors, depending on the elevation and the region investigated (between 0 m and 1000 m for Scandinavia, a lower elevation range than for the French Alps).

To the best of our knowledge, few studies have so far shown such a significantly lower cold bias over mountainous regions between a RCM and a CP-RCM . Nevertheless, the generalized RCM cold biases in the Alps has led to some hypotheses that could be used to explain the lower cold bias observed. Kotlarski et al. (2014); Vautard et al. (2013) invoked the persistence of a too extended snow cover in the RCMs, which would lead to a cooling during the winter months due to the interaction of snow-covered soils and the atmosphere. They also pointed out potential issues in the parameterization of the surface scheme leading to insufficiently strong ablation processes (melt, etc.) of the snow cover. A too persistent snow cover is also invoked in Kevin et al. (2017) which investigateed the effects of snow albedo feedback on the temperature at 2 m, although in this study the ALADIN model was the only model appearing to be insensitive to the snow albedo feedback.

Keller et al. (2016) and Ban et al. (2014) stated that a better representation of clouds linked to the explicit resolution of deep convection, modifying the surface radiation balance, could provide more realistic temperature diurnal extrema.

Other hypotheses are discussed in the following section.

| AROME vs. S2M and ADAMONT

Despite the lower cold bias of AROME compared to ALADIN, AROME output provides lower temperature than in the S2M reanalysis or ADAMONT adjusted projections, especially in winter and spring at high elevations in past or future climate. Although part of the cold bias could be inherited from ALADIN, this does not seem to explain it entirely, since it is also found in NWP applications of AROME as highlighted by Vionnet et al. (2016), who compared the operational AROME NWP surface atmospheric fields with the S2M reanalysis over 4 winters (2011 to 2014). According to Vionnet et al. (2016) and Quéno et al. (2020), this cold bias could be due to the underestimation of downward infrared radiation (ILW), and the overestimation of incident solar radiation (ISW) in AROME, related to an underestimation of the cloud cover.

The snow cover model and its interaction with the atmosphere in AROME may also play a role. Indeed, the single-layer scheme describing the evolution of the snow cover in AROME (D95, Douville et al. (1995)) does not simulate liquid water retention in the snow cover, and the influence of freezing/thawing on surface latent fluxes. According to Vionnet et al. (2016), this absence can lead to an underestimation of the surface temperature, by omitting the surface refreezing processes releasing latent heat by phase change. This process is particularly active during melting periods, and may explain the stronger deviation from December to May. Finally, Rontu et al. (2016) have also suggested that the turbulence scheme in AROME may misrepresent stable boundary layer dynamics, leading to an underestimation of mixing, and thus to a too frequent decoupling of the surface and the atmosphere. The decoupling leading to lower near surface temperatures and snow surface temperatures is also an hypothesis put forward by Lapo et al. (2015), who compared the response of two snow models of different complexity to irradiance errors.

By gathering together literatures, some hypotheses can be retained to partly explain the cold biases over the Alps, whether they come from RCMs or CPRCMs :

- A too thick and persistent snow cover in the RCM and possibly the CP-RCM combined with a too coarse representation of the topography.
- Problems related to the parameterizations, impacting the representation of turbulent fluxes and the too simple snow cover scheme in AROME.
- Incorrect representation of the cloud cover, leading to a biased radiation balance.

Further studies are needed to investigate these issues through sensitivity studies, focusing on the parameterizations mentioned above, in similar configurations in order to apportion the contribution to the total bias due to each of the parameterizations, and the part inherited from the driving models.

Overall, these hypotheses help to better understand the observed cold bias between AROME and the S2M reanalysis. They may also be invoked to explain part of the cold bias of the ALADIN RCM, and help understanding the processes behind the unrealistic snow accumulation shown in Figures 4-d-h.

| Spurious snow accumulation

As shown in Figure 4.d-h 6.h-p and described in section 3, snow accumulates irrealistically at some grid points, for AROME driven by ERAi above 2100 m, from 1500 m when driven by CNRM-CM5, and above 2400 m for ALADIN driven by ERAi, 2100 m when driven by CNRM-CM5.

Above 2500 m, it is expected for snow to accumulate from one year to the next, since this elevation corresponds to the lower limit of the equilibrium elevation line of the Alpine glaciers, on average around 3000 m (Rabatel et al., 2013). The S2M reanalysis, which focuses on seasonal snow, is designed to partly reset the snow cover state on August 1^{st} each year in order to limit multiannual snow accumulation (Vernay et al., 2021). However, below 2500 m, it is unrealistic for snow to accumulate from one year to the next, and reflects an erroneous behaviour of the corresponding model.

We note that snow accumulates more and at lower elevations when driven by the CNRM-CM GCM than by ERAi in ALADIN and AROME. This behavior is similar to what was identified in the studies investigating the results of the EURO-CORDEX RCMs by Terzago et al. (2017), focusing on the snow water equivalent (SWE) and Matiu et al. (2020) focusing on the snow cover fraction and snow depth. In these two studies, the authors attribute the differences in accumulation to atmospheric forcings (as a "legacy" of GCM biases), inducing a thicker snowpack (due to higher snowfall and lower temperatures). This hypothesis is consistent with our results, as snowfall (total precipitation and fraction of solid precipitation) for AROME and ALADIN (and air temperature for AROME) are significantly higher when driven by a GCM than driven by ERAi (see table 1) and could therefore explain differences between ERAi and GCM driven simulations.

However, as snowfall amount and air temperature at 2 meters values are respectively higher and lower in ALADIN outputs, neither the atmospheric forcings (from the GCM), nor the atmospheric conditions within ALADIN or AROME can explain the highest snow accumulation found in AROME outputs, in past or future climate.

Some further explanations for this behaviour are hypothesized and listed below :

- The different degrees of complexity of the snowpack scheme used in each model probably participate to the difference in snow accumulation. AROME uses D95 model which is a single-layer snowpack scheme coupled within

AROME, while ALADIN uses the multi-layer ISBA-ES model, taking into account more processes than D95 such as the liquid water retention, heat transfer, compaction, and thawing/freezing latent fluxes.

- The differences in the radiation balance as well as the turbulence parameterizations affect near surface conditions.
- The daily/hourly characteristics of wet events as well as differences in temperatures diurnal cycles (intensities, durations and frequencies) may affect the responses of the snowpack scheme and explain part of the more or less pronounced snow accumulation between models, congurations and between grid points for a given model and configurations.
- According to Terzago et al. (2017), more finely resolved topography allows areas of snow accumulation to be better isolated, and thus produce stronger maxima, corresponding to mountain peaks.

In summary, spurious snow accumulation below 2500 m might be explained by the atmospheric conditions (higher snowfall, cold biases, daily/hourly characteristics of wet events, and diurnal cycle of temperatures), weaknesses of the snowpack schemes (and their different levels of complexity) and the surface-atmosphere coupling (snow albedo feedback, radiation/turbulence paramterizations). All of these factors vary among configurations and models, explaining differences in snow accumulation between models simulations.

Addressing the causes for spurious snow accumulation would require further studies to apportion the contribution of the different factors involved and improve the models accordingly.

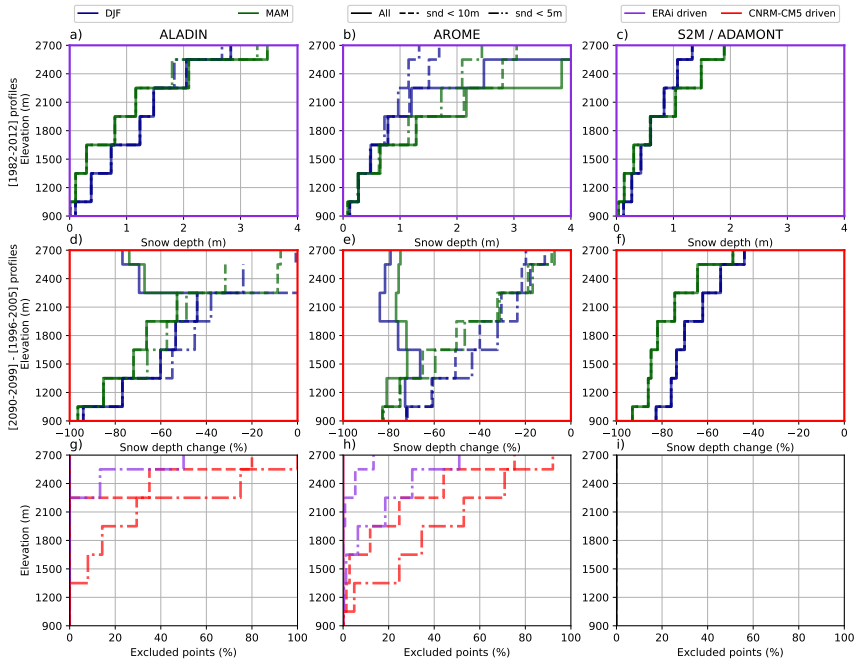

FIGURE 8 Altitudinal profiles of mean snow depth (snd) values averaged over the 1982-2012 period for DJF and MAM seasons for ALADIN (a), AROME (b) and S2M (c), with different threshold values applied to exclude grid points exceeding the threshold values from the profiles (no threshold - solid line, 10 meters - dashed line, 5 meters - dotted line). The second line shows the difference of mean snow depth values for DJF and MAM seasons, between the averages of the end-of-century (2090-2099) and beginning-of-century (1996-2005) period for ALADIN (d), AROME (e), ADAMONT (f) with same thresholds applied than for panels a), b) and c). The third line shows the proportion of points excluded according to each threshold (dashed line - 10 meters, dotted line - 5 meters), respectively for panels a), b) and c) in violet, and for panels d), e) and f) in red.

Figures 5 and 7 (and Figures A2 and A4) show that snow accumulation only concerns some grid points for AROME and ALADIN, with high values bringing the spatial averages to exceptionnally high values at high elevations (see Figures 4.d-h and 6.h-p).

Figure 8 shows the altitudinal profiles of mean snow depth values for DJF and MAM seasons, similar to Figure 4.d (for ALADIN, AROME and S2M) and Figure 6.d-l (for ALADIN, AROME and ADAMONT), but excluding some grid points from the computation according to different snow depth thresholds. Thresholds are applied to seasonal means, in such a way that if a seasonal value at a given grid point (or S2M elevation band) exceeds the threshold for at least one year for one season, the grid point is entirely removed from the computation of the spatial average for a given elevation band.

Figure 8.a-b shows that using a 5 m threshold reduces the deviation above 2400 m between ALADIN and S2M, and between AROME and S2M above 2100 m. The number of excluded points is larger for AROME than for ALADIN in Figure 8.g-h, because the spurious snow accumulation pattern concerns more grid points in AROME simulations (30% at 2400 m for the 5 m threshold) than in ALADIN outputs (only 15% at 2400 m for the 5 m threshold), whereas no elevation bands are removed from S2M simulations (see Figure 8.i). Figure 8.a-b also shows that despite the lower deviation above 2100 m for AROME and ALADIN with a 5 m threshold, both are still showing higher snow depth values than S2M for both seasons and all elevation bands. These results are consistent with the hypotheses provided above to explain snow accumulation, due to too high snowfall values, and underestimated snowmelt, leading to generally overestimating snow depth values in AROME and ALADIN.

Figure 8.g-h also confirms that snow accumulation is larger and more extended geographically in simulations driven by CNRM-CM5 than by ERAi, with more than twice the number of excluded points for AROME regardless of the elevations considered, and more than 3 times in ALADIN at 2400 m for the 5 m threshold.

Figure 8.d-e shows that applying a 5 m threshold considerably modifies the shape of the elevation profile for both seasons, and better matches the relative decrease with elevation of the snowdepth decrease of the ADAMONT data results across the 21^{st} century. Nevertheless, for both AROME and ALADIN, results above 2100 m when driven with CNRM-CM5 are obtained using less than 40% of the grid points, that are not removed, thereby questioning the representativeness of this result.

Overall, even if snow depth values as they stand are difficult to exploit at high elevation for AROME and ALADIN and can affect the overall simulation results due to snow cover feedbacks, removing the grid points concerned by exceptionnal snow accumulation may enable a restricted use of the snow depth fields. We note that these problems are not systematically encountered for all CP-RCMs (Lüthi et al., 2019).

| Difference in future climate change between dynamic and statistical downscaling

By design, ADAMONT cannot represent elevation-dependent warming, because for each massif only one grid point from the driving RCM is used (Verfaillie et al., 2017; Pepin et al., 2015), in contrast to AROME which intrinsically represents the topography at 2.5 km horizontal resolution. The vertical distribution of summer and autumn warming rates could be interpreted as indicating an elevation-dependent warming signal, but an investigation of the distribution of grid points for AROME at differents elevations (see Figures A3 and A4) partly dismisses this hypothesis at least at the scale of the French Alps. Indeed, the distribution of grid points at high elevations are not well distributed among the French Alps, but concentrated in inner Alps in constrast to low elevations with more points concentrated in exterior

Alps. Therefore, regionally aggregated elevation dependent warming could actually reflect spatial variations of the warming rate. The temperature change in the AROME and ALADIN outputs show a rather smooth spatial pattern, while ADAMONT shows a larger inter-massif variability, potentially inherited from S2M heterogeneities used for the adjustement process. A stronger warming signal than AROME are also found in ADAMONT for the summer and spring seasons at all elevations and the autumn below 1800 m.

Similar geographical variations of the 21^{st} century change in the amount of seasonal precipitation in the French Alps can be seen in all three datasets : general increase in winter and autumn in the northern part at all elevations, and a decrease in the southern part at all elevation, whereas a general drying dominates in spring and summer in the entire domain. Investigations were conducted by Ménégoz et al. (2020) addressing 20^{th} century changes in the French Alps using the MAR model driven by a reanalysis, where wetter trends were explained by more intense wet days and longer albeit less-frequent wet spells, and drying trends with less frequent wet days. Further extensive research at finer spatio-temporal scale would provide further information on these changes. Despite close geographical variation, the AROME simulations almost systematically show either a larger relative increase or a smaller relative decrease of accumulated precipitations compared to the ADAMONT adjusted projections.

For the fraction of solid precipitation in winter and the snow depth values at the different elevation investigated, the same analysis as for the accumulated precipitations can be made, with close geographical differences, but a smaller change in AROME and ALADIN compared to ADAMONT, consistent with comparatively lower temperature change.

For all variables considered, the spatial pattern of the changes are generally similar for AROME and ADAMONT. This also holds true for ALADIN although its low horizontal resolution does not allow to represent the finest spatial variations. Differences in the changes remain difficult to interpret, due to the multitude of limitations induced by the two types of downscaling, which can alter the changes, and the difficulty in quantifying the impact of each. Our study shows that both the AROME and ALADIN simulations exhibit large cold deviations compared to ADAMONT outputs, that can reasonably be considered as biases in the evaluation period.

Concerning the ADAMONT statistical adjustment, Verfaillie et al. (2017) recall that the quality of the method when applied outside its learning period depends strongly on the quality and temporal homogeneity of the observations used to carry out the adjustment. However, the SAFRAN S2M reanalysis has spatial and temporal heterogeneities over mountain regions and make the assumption of intra-massif homogeneity which is not systematically verified. Furthermore, Verfaillie et al. (2017) suggest that spatial heterogeneity in the quality of the asjustments may be induced by the method of selecting the points to be used due to a lack of points at high elevation with ALADIN compared to S2M. An additional source of uncertainty for its application in future climate concerns the assumption of temporal invariance of regional climate model errors as well as a modification of the climate change trends due to quantile mapping adjustment (Maraun, 2016).

| On the added value of using CP-RCMs to model past and future climate

Despite all the limitations discussed in the previous sections, the use of CP-RCMs and specifically AROME in this study shows clear added-values compared to raw ALADIN outputs, but also with respect to using the statistical downscaling and adjustment method ADAMONT using S2M as a reference.

Compared to ALADIN outputs, temperature differences between S2M and ADAMONT are lower in AROME simulations, regardless of the seasons and elevation. The hypotheses invoked to explain these lower values are discussed in

section 4. accumulated precipitation values for a given elevation are almost systematically lower in AROME compared to ALADIN, and closer to S2M values used as a reference. Due to the parameterisation of deep convection, the triggering of the convective pattern during orographic uplift may be too frequent and too intense in ALADIN simulations. Prein et al. (2013) showed that most RCMs that do not explicitly resolve deep convection produce convective systems that evolve too slowly, leading to an overestimation of their intensity, net heat transport, and precipitation. Moreover, the ALADIN mesh represents the Alps as a long north-western slope, which flattens the pre-Alpine massifs to the north, and does not allow for an accurate account of the barrier effects leading to low accumulated precipitations in the inner massifs. This largely explains the high accumulations at 1800 m elevation simulated in ALADIN (see Table 1).

On the other hand, the seasonal accumulations values produced by AROME (see Figures 4b-f), showing a strong altitudinal increase, and maxima in winter and spring, are very different from those in S2M in past climate or ADAMONT in future climate for which the altitudinal gradient is lower, with maxima in autumn. These results were also found with MAR simulations compared to S2M reanalyses and other observation datasets Ménégoz et al. (2020), as well as similar geographical seasonal variations of accumulated precipitations. Similarly to the results of Vionnet et al. (2016), we find that total snowfall values are larger for AROME above 1800 m, with a difference increasing with elevation, despite a strong spatial variability relative to the orography. According to Vionnet et al. (2019), the quality of the SAFRAN precipitation reanalysis is limited at high elevations due to the lack of observation stations used in the analysis, and by limitations of precipitation measurements for snowfall due to wind-induced undercatch. These discrepancies over mountain regions between observing systems and CP-RCMs have already been shown with the WRF atmospheric model and the PRISM observation dataset in the USA by Hughes et al. (2020), who also noted that models systematically overestimate precipitations on the windward side of mountains, and underestimate them on the lee side. Although these investigations only concern snow precipitation, they make it possible to explain, on the one hand, the increase in the difference in accumulations with elevation and, on the other hand, the difference between AROME and S2M in terms of the seasonal maximum accumulations, in autumn for S2M and the November to April period for AROME.

Despite the difficulty of drawing conclusions due to the absence of fully reliable observation sources at high elevations, it is possible that the accumulations simulated by AROME in the high mountains are closer to reality than those of S2M, and by design, those of ADAMONT.

Overall, assessments using several sets of observations, as performed by (Ménégoz et al., 2020) at finer spatio-temporal scales, on daily or subdaily indicators, as well as on extremes events, are worth exploring in the future in order to assess another dimension for which CP-RCMs are designed to provide further added value.

5 | CONCLUSION

Simulations of the CP-RCM AROME, driven by the RCM ALADIN under past and future climate conditions, are analyzed in the French Alps, and compared to its driving RCM as well as a statistical downscaling method ADAMONT applied to the same driving RCM. We demonstrated the added value of AROME compared to its driving RCM ALADIN, with temperature and precipitation fields closer to the reference values from the S2M reanalysis. Also, the use of AROME leads to a better representation of the geographical patterns of the variables based on 10 years averages for the historical simulations, as well as on 30 years average. As multiple studies have suggested for high resolution models (Lundquist et al., 2019), AROME could also provides a better estimate of accumulated precipitation at high

elevation than the S2M reanalysis and consequently the ADAMONT projections, which are based on the reanalysis, although this added value remains difficult to assess due to the lack of reliable observations at high elevation. Future projections with AROME show more realistic spatial patterns, for a given elevation, than ADAMONT results, which inherit and potentially amplify, in future projections, spatial heterogeneities from the S2M reanalysis used as a reference dataset. This study corroborates the advantages in the use of CP-RCMs over mountain regions, as Prein et al. (2013) did in their study by showing the systematic added value of CP-RCMs in summer rainfall that we extend here with the other seasonal rainfall, the representation of near-surface temperature fields showing added-value here compared to ALADIN with a smaller negative temperature deviation. The added-values listed above having cascading effects on the estimation of the rain-snow limit elevation, snow precipitation, and snow depth values.

Nevertheless, there are still some obstacles to using AROME to fully exploit all of its output variables. Indeed, strongly negative temperature differences between AROME the simulations and S2M-based simulations at intermediate and high elevations in both past and future climate conditions are remaining, appearing as a recurrent feature of AROME simulations. Preliminary investigations suggest that it is linked to its representation of surface radiative fluxes, to the coupling with its surface model, and thus to its capacity to correctly represent the surface-atmosphere interactions, in particular concerning the evolution of the snow cover. Unrealistic accumulation of snow is also found at elevation above 1800 m, and is most probably the result of several factors, that we expect some to be partly linked with the cold bias, and that affect only some grid points at a problematic amplitude. These need to be extensively studied and addressed, but provided that grid points characterized by spurious snow cover accumulation in AROME and ALADIN simulations are removed from the analysis, snow depth fields from these simulations are consistent with S2M/ADAMONT simulations, with differences requiring further investigations.

Some characteristics at finer spatial and temporal scales of the CP-RCMs outputs remain to be studied in mountain areas and constitute promising perspectives to be explored. Indeed Prein et al. (2020) highlighted the benefits of CP-RCMs by their capacity to quantify and represent extreme events. Matiu et al. (2020) expected that the finer resolution would increase precision of the temperature fields and orography, also improving the representation of the hydrological phenomena and the snow cover fields. These potentialities (not addressed here) open up a wide field of research applications in a large number of areas related to the impacts of climate change on mountain social-ecological systems. The use of the AROME CP-RCM to study climate over mountain regions demontrate clear added-value compared to its coarser-scale driving RCM ALADIN, whether it concerns the representation of accumulated precipitations or finer and less biased temperatures fields, both in all seasons. Further benefits are expected concerning the representation of snow conditions (Terzago et al., 2017; Matiu et al., 2020), even if critical issues were identified in AROME.

Besides these improvements, the differences between a dynamic and statistical downscaling of climate change projections remain difficult to assess in detail as both feature limitations, although our study provides a consistent analytical framework for evaluating CP-RCMs outputs in a systematic way. It is therefore necessary, and possible, to complement this study with extensive developments on statistical adjustments, applicable for CP-RCMs, and with multi-model approaches to better quantify the model uncertainties. Nevertheless, the increasing use of CP-RCMs in the assessment of climate change impacts through various European and international projects (e.g. CORDEX Flagship Pilot Study - Convection (Coppola et al., 2020; Ban et al., 2021; Pichelli et al., 2021)) as well as the particular attention given to mountain regions (TEAMx, Rotach et al. (2020)) are encouraging perspectives for future research in this field.

Acknowledgments

The authors gratefully acknowledge the WCRP-CORDEX-FPS on Convective phenomena at high resolution over Europe and the Mediterranean [FPSCONV-ALP-3]. This work is part of the Med-CORDEX initiative (http://www.medcordex.eu). CNRM/CEN is part of LabEX OSUG@2020. We acknowledge the work of two anonymous reviewers, who provided relevant feedback and suggestions and contributed to improve the original manuscript.

References

Ban, N., Caillaud, C., Coppola, E., Pichelli, E., Sobolowski, S., Adinolfi, M., Ahrens, B., Alias, A., Anders, I., Bastin, S. et al. (2021) The first multi-model ensemble of regional climate simulations at kilometer-scale resolution, part i: evaluation of precipitation. *Climate Dynamics*, 1–28.

Ban, N., Schmidli, J. and Schär, C. (2014) Evaluation of the convection-resolving regional climate modeling approach in decade-long simulations. *Journal of Geophysical Research: Atmospheres*, **119**, 7889–7907.

Bénard, P., Vivoda, J., Mašek, J., Smolíková, P., Yessad, K., Smith, C., Brožková, R. and Geleyn, J.-F. (2010) Dynamical kernel of the Aladin–NH spectral limited-area model: Revised formulation and sensitivity experiments. *Quarterly Journal of the Royal Meteorological Society*, **136**, 155–169.

Beniston, M., Farinotti, D., Stoffel, M., Andreassen, L. M., Coppola, E., Eckert, N., Fantini, A., Giacona, F., Hauck, C., Huss, M., Huwald, H., Lehning, M., López-Moreno, J.-I., Magnusson, J., Marty, C., Morán-Tejéda, E., Morin, S., Naaim, M., Provenzale, A., Rabatel, A., Six, D., Stötter, J., Strasser, U., Terzago, S. and Vincent, C. (2018) The European mountain cryosphere: a review of its current state, trends, and future challenges. *The Cryosphere*, **12**, 759–794.

Boone, A. and Etchevers, P. (2001) An intercomparison of three snow schemes of varying complexity coupled to the same land surface model: Local-scale evaluation at an Alpine site. *Journal of Hydrometeorology*, **2**, 374–394.

Caillaud, C., Somot, S., Alias, A., Bernard-Bouissières, I., Fumière, Q., Laurantin, O., Seity, Y. and Ducrocq, V. (2021) Modelling mediterranean heavy precipitation events at climate scale: an object-oriented evaluation of the cnrm-arome convection-permitting regional climate model. *Climate Dynamics*, **56**, 1717–1752.

Coppola, E., Sobolowski, S., Pichelli, E., Raffaele, F., Ahrens, B., Anders, I., Ban, N., Bastin, S., Belda, M., Belusic, D. et al. (2020) A first-of-its-kind multi-model convection permitting ensemble for investigating convective phenomena over Europe and the Mediterranean. *Climate Dynamics*, **55**, 3–34.

Decharme, B., Brun, E., Boone, A., Delire, C., Le Moigne, P. and Morin, S. (2016) Impacts of snow and organic soils parameterization on northern Eurasian soil temperature profiles simulated by the ISBA land surface model. *The Cryosphere*, **10**, 853–877.

Decharme, B., Delire, C., Minvielle, M., Colin, J., Vergnes, J.-P., Alias, A., Saint-Martin, D., Séférian, R., Sénési, S. and Voldoire, A. (2019) Recent changes in the ISBA-CTRIP land surface system for use in the CNRM-CM6 climate model and in global off-line hydrological applications. *Journal of Advances in Modeling Earth Systems*, **11**, 1207–1252.

Dee, D. P., Uppala, S. M., Simmons, A., Berrisford, P., Poli, P., Kobayashi, S., Andrae, U., Balmaseda, M., Balsamo, G., Bauer, d. P. et al. (2011) The ERA-Interim reanalysis: Configuration and performance of the data assimilation system. *Quarterly Journal of the royal meteorological society*, **137**, 553–597.

Déqué, M., Alias, A., Somot, S. and Nuissier, O. (2016) Climate change and extreme precipitation: the response by a convection-resolving model. *Research activities in atmospheric and oceanic modelling CAS/JSC working group on numerical experimentation. Report*.

Douville, H., Royer, J.-F. and Mahfouf, J.-F. (1995) A new snow parameterization for the Meteo-France climate model. *Climate Dynamics*, **12**, 21–35.

Durand, Y., Giraud, G., Laternser, M., Etchevers, P., Mérindol, L. and Lesaffre, B. (2009) Reanalysis of 47 years of climate in the french alps (1958–2005): climatology and trends for snow cover. *Journal of Applied Meteorology and Climatology*, **48**, 2487–2512.

Evin, G., Hingray, B., Blanchet, J., Eckert, N., Morin, S. and Verfaillie, D. (2019) Partitioning uncertainty components of an incomplete ensemble of climate projections using data augmentation. *Journal of Climate*, **32**, 2423–2440.

Frei, P., Kotlarski, S., Liniger, M. A. and Schär, C. (2018) Future snowfall in the alps: projections based on the euro-cordex regional climate models. *The Cryosphere*, **12**, 1–24.

Fumière, Q., Déqué, M., Nuissier, O., Somot, S., Alias, A., Caillaud, C., Laurantin, O. and Seity, Y. (2020) Extreme rainfall in mediterranean france during the fall: added value of the CNRM-AROME Convection-Permitting Regional Climate Model. *Climate Dynamics*, **55**, 77–91.

Giorgi, F., Torma, C., Coppola, E., Ban, N., Schär, C. and Somot, S. (2016) Enhanced summer convective rainfall at Alpine high elevations in response to climate warming. *Nature Geoscience*, **9**, 584–589.

Hock, R., Rasul, R., Adler, C., Cáceres, B., Gruber, S., Hirabayashi, Y., Jackson, M., Kääb, A., Kang, S., Kutuzov, S., Milner, A., Molau, U., Morin, S., Orlove, B. and Steltzer, H. (2019) High Mountain Areas. In *IPCC Special Report on the Ocean and Cryosphere in a Changing Climate* (eds. H.-O. Pörtner, D. Roberts, V. Masson-Delmotte, P. Zhai, M. Tignor, E. Poloczanska, K. Mintenbeck, A. Alegriáa, M. Nicolai, A. Okem, J. Petzold, B. Rama and N. Weyer), 131–202. .

Hughes, M., Lundquist, J. D. and Henn, B. (2020) Dynamical downscaling improves upon gridded precipitation products in the sierra nevada, california. *Climate Dynamics*, **55**, 111–129.

Jacob, D., Petersen, J., Eggert, B., Alias, A., Christensen, O. B., Bouwer, L. M., Braun, A., Colette, A., Deque, M., Georgievski, G., Georgopoulou, E., Gobiet, A., Menut, L., Nikulin, G., Haensler, A., Hempelmann, N., Jones, C., Keuler, K., Kovats, S., Kroner, N., Kotlarski, S., Kriegsmann, A., Martin, E., Meijgaard, E. V., Moseley, C., Pfeifer, S., Preuschmann, S., Radermacher, C., Radtke, K., Rechid, D., Rounsevell, M., Samuelsson, P., Somot, S., Soussana, J.-F., Teichmann, C., Valentini, R., Vautard, R., Weber, B. and Yiou, P. (2014) EURO-CORDEX: new high-resolution climate change projections for European impact research. *Regional Environmental Change*, **14**, 563–578.

Keller, M., Fuhrer, O., Schmidli, J., Stengel, M., Stöckli, R. and Schär, C. (2016) Evaluation of convection-resolving models using satellite data: The diurnal cycle of summer convection over the alps. *Meteorologische Zeitschrift*, **25**, 165–179.

Kevin, J.-P. W., Kotlarski, S., Scherrer, S. C. and Schär, C. (2017) The alpine snow-albedo feedback in regional climate models. *Climate dynamics*, **48**, 1109–1124.

Kotlarski, S., Keuler, K., Christensen, O. B., Colette, A., Déqué, M., Gobiet, A., Goergen, K., Jacob, D., Lüthi, D., Van Meijgaard, E. et al. (2014) Regional climate modeling on european scales: a joint standard evaluation of the euro-cordex rcm ensemble. *Geoscientific Model Development*, **7**, 1297–1333.

Kotlarski, S., Lüthi, D. and Schär, C. (2015) The elevation dependency of 21st century European climate change: an RCM ensemble perspective. *International Journal of Climatology*, **35**, 3902–3920.

Lapo, K. E., Hinkelman, L. M., Raleigh, M. S. and Lundquist, J. D. (2015) Impact of errors in the downwelling irradiances on simulations of snow water equivalent, snow surface temperature, and the snow energy balance. *Water resources research*, **51**, 1649–1670.

Lind, P., Belušić, D., Christensen, O. B., Dobler, A., Kjellström, E., Landgren, O., Lindstedt, D., Matte, D., Pedersen, R. A., Toivonen, E. et al. (2020) Benefits and added value of convection-permitting climate modeling over fenno-scandinavia. *Climate Dynamics*, **55**, 1893–1912.

Lind, P., Lindstedt, D., Kjellström, E. and Jones, C. (2016) Spatial and temporal characteristics of summer precipitation over central Europe in a suite of high-resolution climate models. *Journal of Climate*, **29**, 3501–3518.

Lundquist, J., Hughes, M., Gutmann, E. and Kapnick, S. (2019) Our skill in modeling mountain rain and snow is bypassing the skill of our observational networks. *Bulletin of the American Meteorological Society*, **100**, 2473–2490.

Lüthi, S., Ban, N., Kotlarski, S., Steger, C. R., Jonas, T. and Schär, C. (2019) Projections of Alpine Snow-Cover in a High-Resolution Climate Simulation. *Atmosphere*, **10**, 463.

Maraun, D. (2016) Bias correcting climate change simulations-a critical review. *Current Climate Change Reports*, **2**, 211–220.

Martin, E. (2005) *Modélisation du manteau neigeux et applications dans les domaines du changement climatique et de l'hydrologie*. Ph.D. thesis.

Matiu, M., Petitta, M., Notarnicola, C. and Zebisch, M. (2020) Evaluating snow in euro-cordex regional climate models with observations for the european alps: Biases and their relationship to orography, temperature, and precipitation mismatches. *Atmosphere*, **11**, 46.

Ménégoz, M., Valla, E., Jourdain, N. C., Blanchet, J., Beaumet, J., Wilhelm, B., Gallée, H., Fettweis, X., Morin, S. and Anquetin, S. (2020) Contrasting seasonal changes in total and intense precipitation in the european alps from 1903 to 2010. *Hydrology and Earth System Sciences*, **24**, 5355–5377.

Morin, S., Samacoïts, R., François, H., Carmagnola, C. M., Abegg, B., Demiroglu, O. C., Pons, M., Soubeyroux, J.-M., Lafaysse, M., Franklin, S. et al. (2021) Pan-european meteorological and snow indicators of climate change impact on ski tourism. *Climate Services*, **22**, 100215.

Nabat, P., Somot, S., Cassou, C., Mallet, M., Michou, M., Bouniol, D., Decharme, B., Drugé, T., Roehrig, R. and Saint-Martin, D. (2020) Modulation of radiative aerosols effects by atmospheric circulation over the euro-mediterranean region. *Atmospheric Chemistry and Physics*, **20**, 8315–8349.

Pepin, N., Bradley, R. S., Diaz, H., Baraër, M., Caceres, E., Forsythe, N., Fowler, H., Greenwood, G., Hashmi, M., Liu, X. et al. (2015) Elevation-dependent warming in mountain regions of the world. *Nature climate change*, **5**, 424–430.

Pichelli, E., Coppola, E., Sobolowski, S., Ban, N., Giorgi, F., Stocchi, P., Alias, A., Belušić, D., Berthou, S., Caillaud, C. et al. (2021) The first multi-model ensemble of regional climate simulations at kilometer-scale resolution part 2: historical and future simulations of precipitation. *Climate Dynamics*, **56**, 3581–3602.

Piriou, J.-M. and Guérémy, J.-F. (2016) Prognostic Condensates Microphysics and Transport A new convection scheme for the global Climate and NWP model ARPEGE.

Prein, A., Gobiet, A., Suklitsch, M., Truhetz, H., Awan, N., Keuler, K. and Georgievski, G. (2013) Added value of convection permitting seasonal simulations. *Climate Dynamics*, **41**, 2655–2677.

Prein, A. F., Rasmussen, R., Castro, C. L., Dai, A. and Minder, J. (2020) Advances in convection-permitting climate modeling.

Quéno, L., Karbou, F., Vionnet, V. and Dombrowski-Etchevers, I. (2020) Satellite-derived products of solar and longwave irradiances used for snowpack modelling in mountainous terrain. *Hydrology & Earth System Sciences*, **24**.

Rabatel, A., Letréguilly, A., Dedieu, J.-P. and Eckert, N. (2013) Changes in glacier equilibrium-line altitude in the western Alps from 1984 to 2010: evaluation by remote sensing and modeling of the morpho-topographic and climate controls. *The Cryosphere*, **7**, 1455–1471.

Radu, R., Déqué, M. and Somot, S. (2008) Spectral nudging in a spectral regional climate model. *Tellus A: Dynamic Meteorology and Oceanography*, **60**, 898–910.

Rontu, L., Wastl, C. and Niemelä, S. (2016) Influence of the details of topography on weather forecast–evaluation of HARMONIE experiments in the Sochi Olympics domain over the Caucasian mountains. *Frontiers in Earth Science*, **4**, 13.

734 Rotach, M. W., Arpagaus, M., Colfescu, I., Cuxart, J., De Wekker, S. F., Evans, M. J., Grubišic, V., Kalthoff, N., Karl, T., Kirsh-
735 baum, D. J. et al. (2020) Multi-scale transport and exchange processes in the atmosphere over mountains. Programme and
736 experiment.

737 Rottler, E., Kormann, C., Francke, T. and Bronstert, A. (2019) Elevation-dependent warming in the Swiss Alps 1981–2017:
738 Features, forcings and feedbacks. *International Journal of Climatology*, **39**, 2556–2568.

739 Ruti, P. M., Somot, S., Giorgi, F., Dubois, C., Flaounas, E., Obermann, A., Dell'Aquila, A., Pisacane, G., Harzallah, A., Lombardi,
740 E. et al. (2016) MED-CORDEX initiative for Mediterranean climate studies. *Bulletin of the American Meteorological Society*,
741 **97**, 1187–1208.

742 Seity, Y., Brousseau, P., Malardel, S., Hello, G., Bénard, P., Bouttier, F., Lac, C. and Masson, V. (2011) The AROME-France
743 convective-scale operational model. *Monthly Weather Review*, **139**, 976–991.

744 Smiatek, G., Kunstmann, H. and Senatore, A. (2016) Euro-cordex regional climate model analysis for the greater alpine region:
745 Performance and expected future change. *Journal of Geophysical Research: Atmospheres*, **121**, 7710–7728.

746 Spandre, P., François, H., Verfaillie, D., Lafaysse, M., Déqué, M., Eckert, N., George, E. and Morin, S. (2019) Climate controls
747 on snow reliability in french alps ski resorts. *Scientific reports*, **9**, 1–9.

748 Spiridonov, V., Déqué, M. and Somot, S. (2005) ALADIN-CLIMATE: from the origins to present date. *ALADIN Newsletter*, **29**,
749 89–92.

750 von Storch, H., Langenberg, H. and Feser, F. (2000) A spectral nudging technique for dynamical downscaling purposes. *Monthly*
751 *weather review*, **128**, 3664–3673.

752 Termonia, P., Fischer, C., Bazile, E., Bouyssel, F., Brožková, R., Bénard, P., Bochenek, B., Degrauwe, D., Derková, M., El Khatib,
753 R., Hamdi, R., Mašek, J., Pottier, P., Pristov, N., Seity, Y., Smolíková, P., Španiel, O., Tudor, M., Wang, Y., Wittmann, C.
754 and Joly, A. (2018) The ALADIN System and its canonical model configurations AROME CY41T1 and ALARO CY40T1.
755 *Geoscientific Model Development*, **11**, 257–281.

756 Terzago, S., Hardenberg, J. v., Palazzi, E. and Provenzale, A. (2017) Snow water equivalent in the alps as seen by gridded data
757 sets, cmip5 and cordex climate models. *The Cryosphere*, **11**, 1625–1645.

758 Uppala, S. M., Kållberg, P., Simmons, A., Andrae, U., Bechtold, V. D. C., Fiorino, M., Gibson, J., Haseler, J., Hernandez, A., Kelly,
759 G. et al. (2005) The ERA-40 re-analysis. *Quarterly Journal of the Royal Meteorological Society: A journal of the atmospheric*
760 *sciences, applied meteorology and physical oceanography*, **131**, 2961–3012.

761 Vautard, R., Gobiet, A., Jacob, D., Belda, M., Colette, A., Déqué, M., Fernández, J., García-Díez, M., Goergen, K., Güttler, I.
762 et al. (2013) The simulation of european heat waves from an ensemble of regional climate models within the euro-cordex
763 project. *Climate Dynamics*, **41**, 2555–2575.

764 Verfaillie, D., Déqué, M., Morin, S. and Lafaysse, M. (2017) The method ADAMONT v1.0 for statistical adjustment of climate
765 projections applicable to energy balance land surface models. *Geoscientific Model Development*, **10**, 4257–4283.

766 Verfaillie, D., Lafaysse, M., Déqué, M., Eckert, N., Lejeune, Y. and Morin, S. (2018) Multi-component ensembles of future
767 meteorological and natural snow conditions for 1500 m altitude in the Chartreuse mountain range, Northern French Alps.
768 *The Cryosphere*, **12**, 1249–1271.

769 Vernay, M., Lafaysse, M., Hagenmuller, P., Nheili, R., Verfaillie, D. and Morin, S. (2019) The S2M meteorological and snow
770 cover reanalysis in the French mountainous areas (1958–present).

771 Vernay, M., Lafaysse, M., Monteiro, D., Hagenmuller, P., Nheili, R., Samacoïts, R., Verfaillie, D. and Morin, S. (2021) The s2m
772 meteorological and snow cover reanalysis over the french mountainous areas, description and evaluation (1958–2020).
773 *Earth System Science Data Discussions*, 1–36.

774 Vionnet, V., Brun, E., Morin, S., Boone, A., Faroux, S., Moigne, P. L., Martin, E. and Willemet, J.-M. (2012) The detailed snowpack
775 scheme crocus and its implementation in surfex v7. 2. *Geoscientific Model Development*, **5**, 773–791.

776 Vionnet, V., Dombrowski-Etchevers, I., Lafaysse, M., Quéno, L., Seity, Y. and Bazile, E. (2016) Numerical weather forecasts at
777 kilometer scale in the French Alps: evaluation and application for snowpack modeling. *Journal of Hydrometeorology*, **17**,
778 2591–2614.

779 Vionnet, V., Six, D., Auger, L., Dumont, M., Lafaysse, M., Quéno, L., Réveillet, M., Dombrowski Etchevers, I., Thibert, E. and
780 Vincent, C. (2019) Sub-kilometer precipitation datasets for snowpack and glacier modeling in alpine terrain. *Frontiers in*
781 *Earth Science*, **7**, 182.

782 Voldoire, A., Sanchez-Gomez, E., y Mélia, D. S., Decharme, B., Cassou, C., Sénési, S., Valcke, S., Beau, I., Alias, A., Chevallier, M.
783 et al. (2013) The CNRM-CM5.1 global climate model: description and basic evaluation. *Climate dynamics*, **40**, 2091–2121.

784 Zekollari, H., Huss, M. and Farinotti, D. (2019) Modelling the future evolution of glaciers in the european alps under the
785 euro-cordex rcm ensemble. *The Cryosphere*, **13**, 1125–1146.

A | APPENDIX

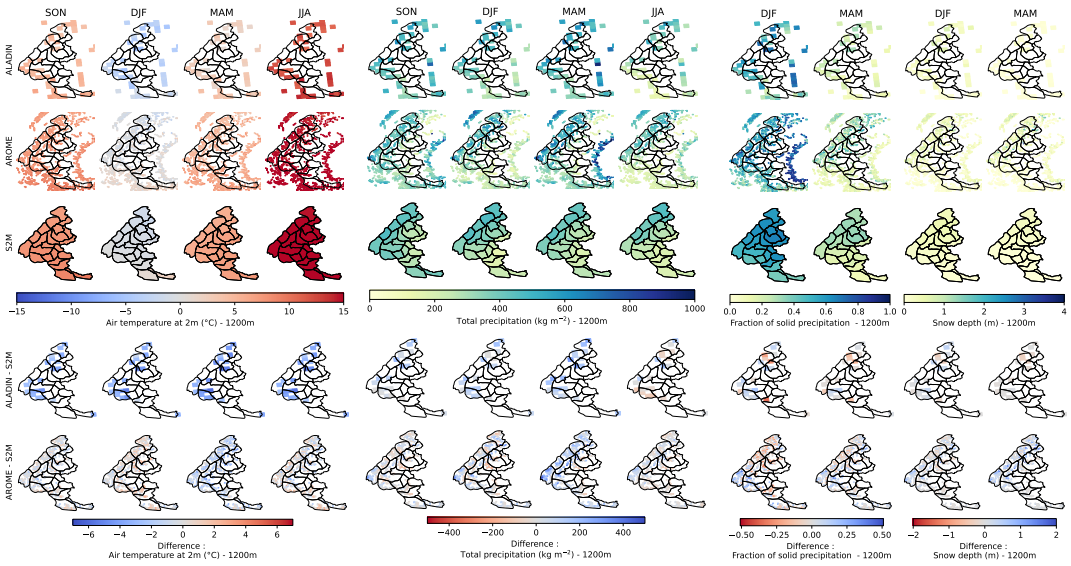

FIGURE A1 Same as Figure 5 but for 1200 m elevation band.

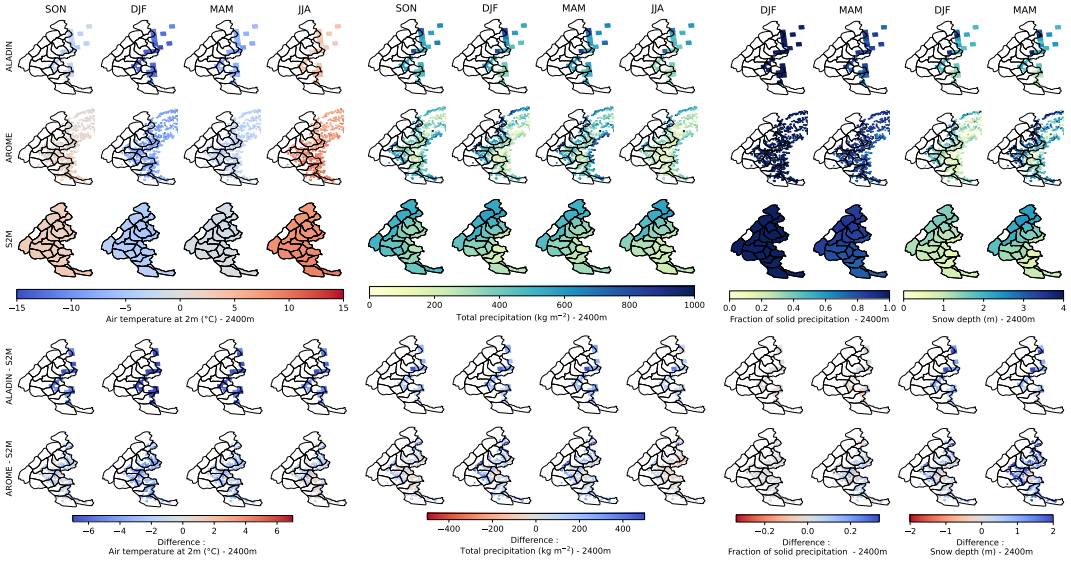

FIGURE A2 Same as Figure 5 but for 2400 m elevation band.

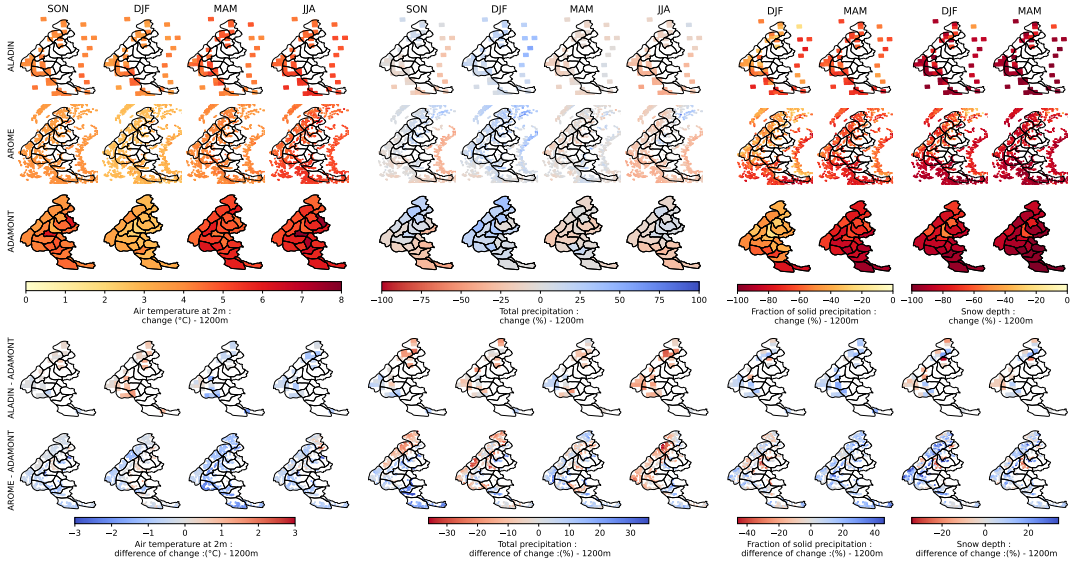

FIGURE A3 Same as Figure 7 but for 1200 m elevation band.

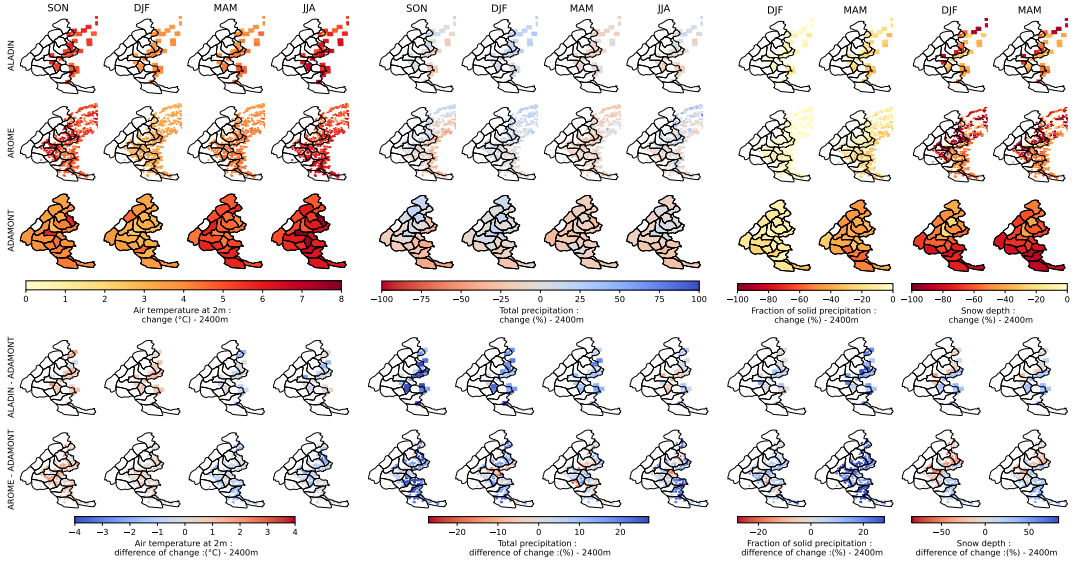

FIGURE A4 Same as Figure 7 but for 2400 m elevation band.